

Supplemental Figure S1



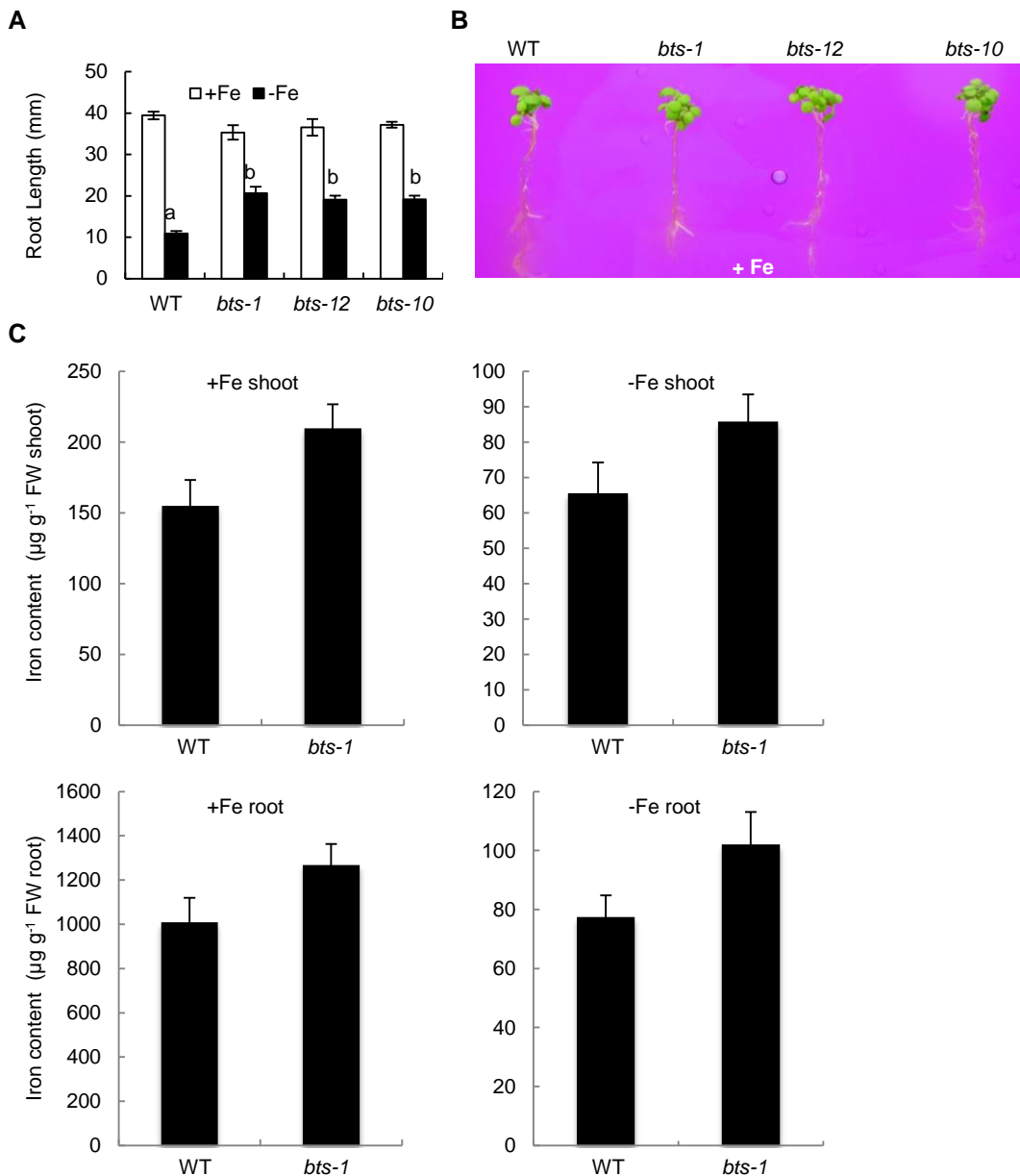
Supplemental Figure S1. GUS activity in wild-type (Col-0) plant. A-D, No GUS expression observed in leaves (A), flower (B), mature green silique (C), and mature embryo. Bars = 5 mm (B and C), 2 mm (D).

Supplemental Figure S2



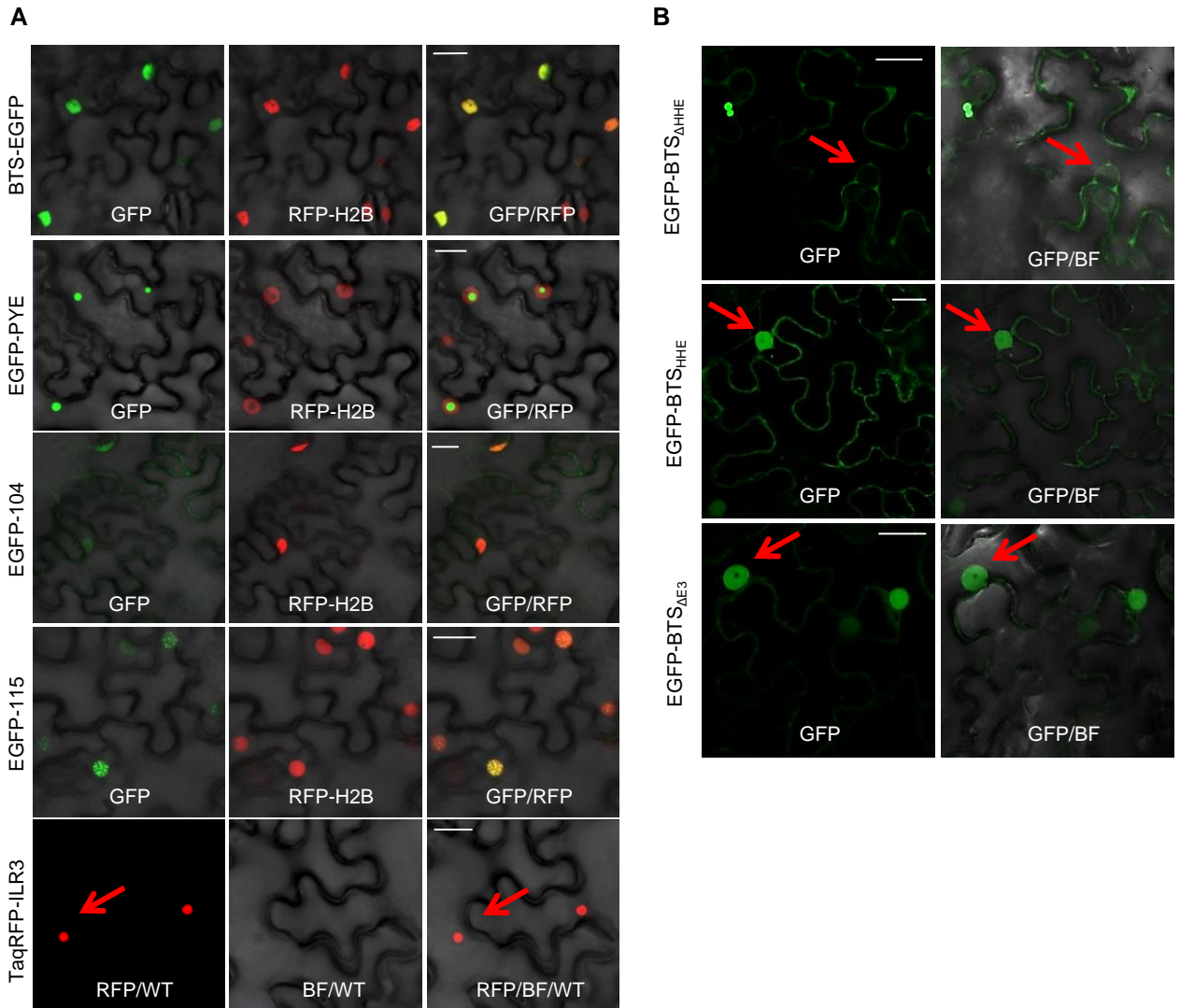
Supplemental Figure S2. Location of *BTS* T-DNA knockdown alleles. Schematic diagram representing position of T-DNA insertions of *bts* alleles.

Supplemental Figure S3



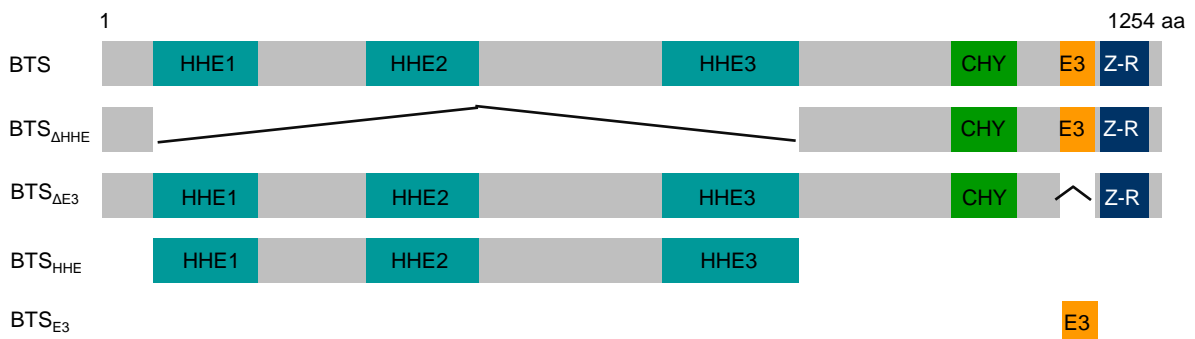
Supplemental Figure S3. Root growth, rhizosphere acidification, and shoot and root iron content in *bts* alleles. A, Root growth of 11-d-old seedlings grown on +Fe media for 4 d and then transferred to \pm Fe media for 7 d (4 d +Fe and 7 d \pm Fe). B, Rhizosphere acidification of 8-d-old seedlings grown on +Fe media (4 d +Fe, 3 d +Fe, and 1 d bromocresol purple). Eight plants per genotype were grouped on bromocresol purple agar media. Results shown represent four independent assays. C, Iron content in shoot and root tissues of 10-d-old wild-type (WT) and *bts-1* seedlings grown on \pm Fe media (7 d +Fe and 3 d \pm Fe). Shoots were washed with deionized water and roots were first desorbed with 2mM CaSO₄ and 10mM EDTA, and then rinsed with deionized water. The elemental analysis were performed by ICP-OES. Error bars indicates \pm SE of the mean (n = 3). FW, Fresh weight.

Supplemental Figure S4



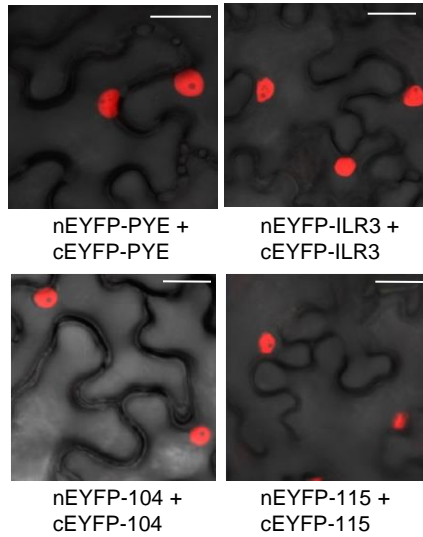
Supplemental Figure S4. Localization of BTS, PYE and PYEL proteins in nucleus. A, EGFP-tagged BTS, PYE, bHLH104, and bHLH115 were transiently expressed in RFP-Histone2B (nuclear marker) transgenic *N. benthamiana* leaves. TaqRFP-ILR3 was expressed in wild-type (WT) *N. benthamiana* leaves. EGFP, RFP and EGFP/RFP overlay images are shown. B, Localization of BTS domains and deletion fragments. EGFP-tagged $BTS_{\Delta HHE}$, BTS_{HHE} , and $BTS_{\Delta E3}$ were transiently expressed in WT *N. benthamiana* leaves. EGFP and EGFP/Bright Field (BF) overlay images are shown. Red arrow points nucleus and nuclear localized protein. Results are representative of three independent experiments. Bars = 20 μm .

Supplemental Figure S5



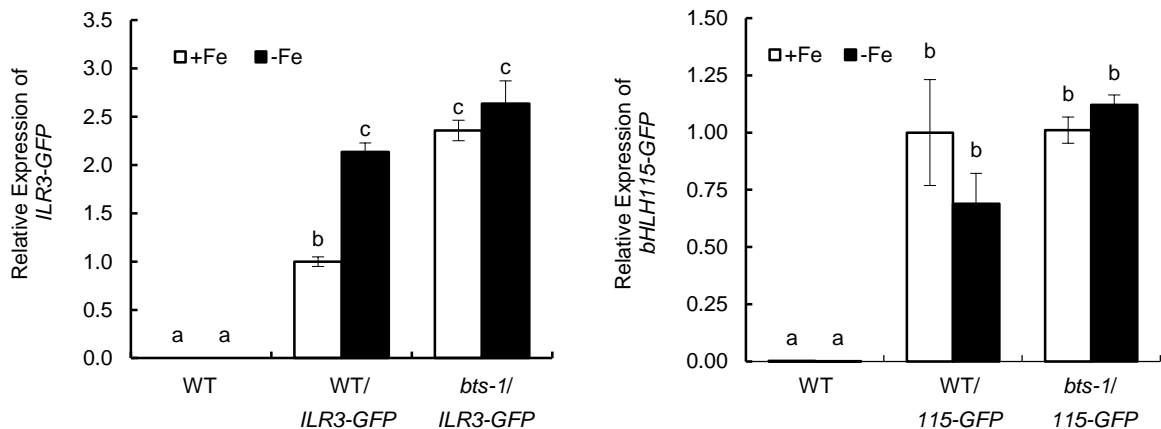
Supplemental Figure S5. Schematic diagram representing BTS protein. The protein structure is predicted by CD-Search (<http://www.ncbi.nlm.nih.gov/Structure/cdd/cdd.shtml>), BTS is predicted to contain three putative iron-binding HHE domains (HHE1_{57-183 aa}, HHE2_{316-445 aa} and HHE3_{666-824 aa}), CHY-type Zn-finger (CHY_{1006-1083 aa}), a RING_{1135-1180 aa} (E3 ligase) domain and putative Zn-Ribbon (Z-R_{1180-1240 aa}) domain. The BTS derivatives (domains and deletion proteins) used for the various biochemical and molecular analysis are shown below the full-length BTS protein structure.

Supplemental Figure S6



Supplemental Figure S6. Lack of PYE and PYEL homodimer formation. BiFC assay for in planta interactions between indicated proteins in the leaf epidermal cells of RFP-Histone2B (nuclear marker) transgenic *N. benthamiana* plants. EYFP/RFP overlay images are shown. Absence of EYFP fluorescence indicates no interaction between indicated proteins. Results are representative of three independent experiments. Bars = 20 μ m.

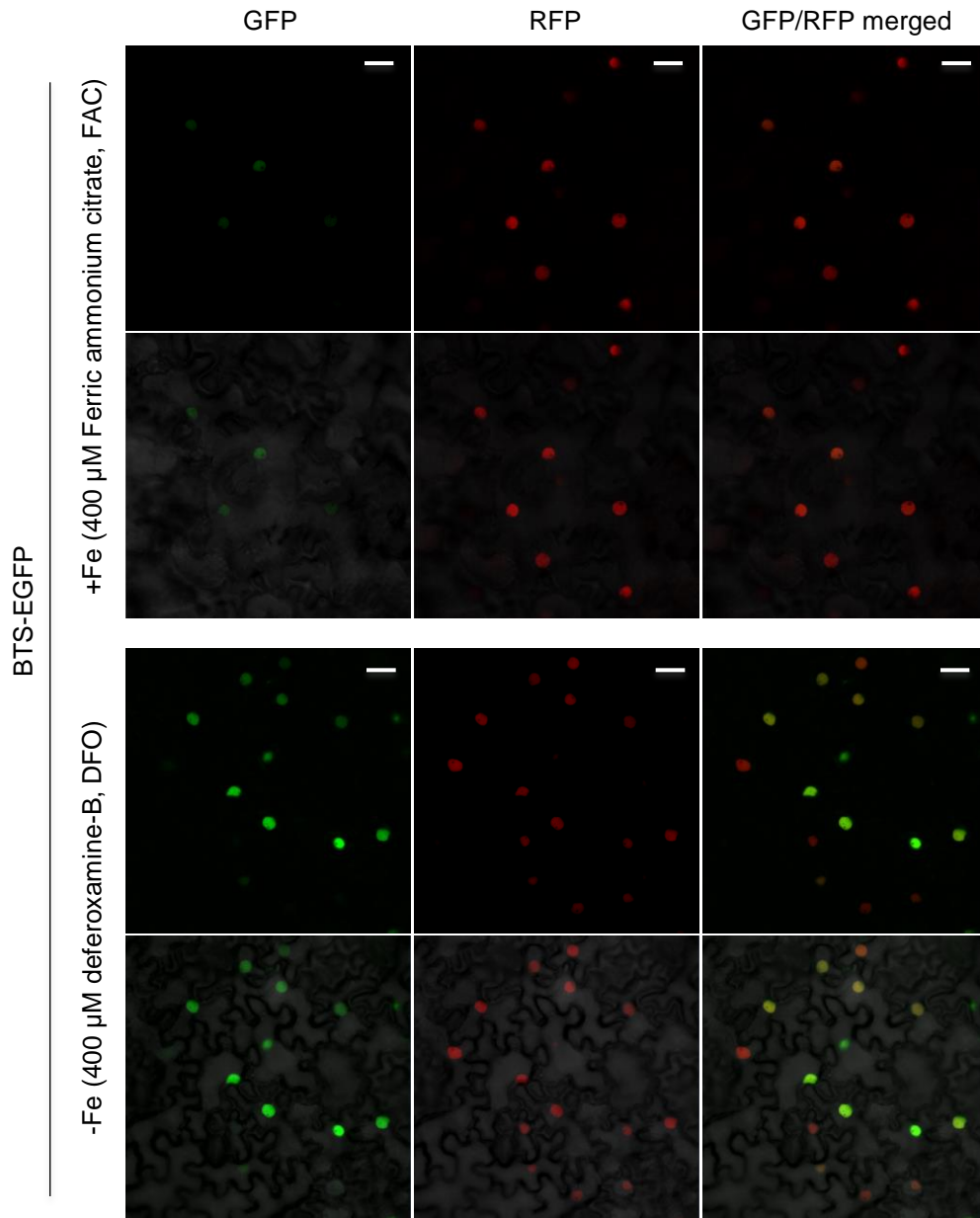
Supplemental Figure S7



Supplemental Figure S7. Relative expression of *ILR3-GFP* and *bHLH115-GFP* in roots. 6-d-old seedlings of wild-type (WT) and *bts-1* mutant expressing *ProILR3::ILR3-GFP* and *Pro115::115-GFP* transgenes, respectively, were grown on +Fe media for 4 d and then transferred to \pm Fe media for 2 d (4 d +Fe and 2 d \pm Fe). Error bars indicate \pm SE of the mean (n = 4), and columns with different letters are significantly different from each other (p<0.05).

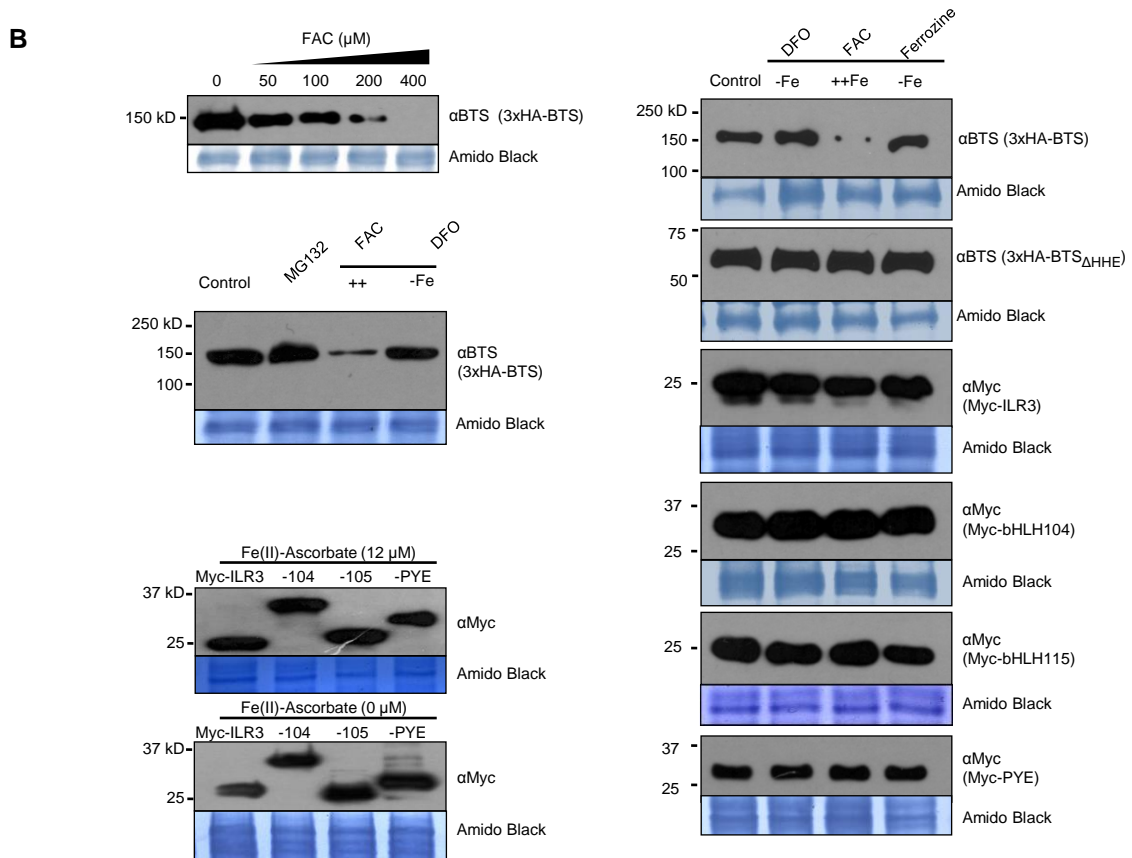
Supplemental Figure S8

A



Supplemental Figure S8. In vivo and in vitro stability of BTS protein in the presence of iron. A, In planta stability of BTS-GFP protein in iron deficient vs sufficient condition. Protein was transiently expressed using the constitutive 35S promoter in RFP-Histone2B transgenic *N. benthamiana* leaves (red nucleus) under iron deficient and sufficient conditions (by infiltrating either 400 μM DFO) and 400 μM ferric ammonium citrate (FAC) respectively, along with agrobacterium infiltration, and visualized by confocal microscopy. The confocal microscope settings were kept same as in Supplemental Fig. S4A to capture the images in order to compare the BTS-EGFP signals due to differential iron treatment. Results are representative of two independent experiments. Bars = 20 μm.

Supplemental Figure S8



Supplemental Figure S8. In vivo and in vitro stability of BTS protein in the presence of iron. B, BTS protein stability is affected by ferric iron (Ferric ammonium citrate, FAC), but not by ferrous iron-chelator (DFO) and 100 μM MG132 (26S proteasomal inhibitor) during in vitro translation using wheat germ extract. Iron does not affect in vitro translation and stability of PYE and PYEL proteins in Fe deficient (400 μM DFO, and 400 μM Ferrozine) and sufficient Fe [ferrous iron, Fe(II)-Ascorbate, or ferric iron, 400 μM FAC] conditions. Amido black staining represents equal amount of in vitro protein translation loaded per lane.

Supplemental Figure S8

C

```

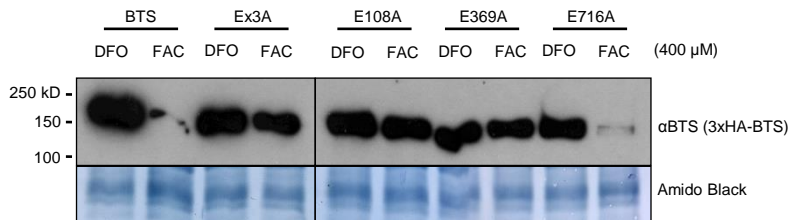
FBXL5 HHE      6  EEVDVFTAPHWRMKQLVGLYCDKLSKTNFS-NNNDFRALLQSLYATFKKEFKMHEQIENEY
BTS HHE1     53  SPILIFLFFHKAVCSEL-EALHRLALEFATGHHVDLRLRLRERYRFLRSIYKHHCNAEDEV
BTS HHE2    313  HPVDEIKLWHKSIKEMKEIADEARKIQLSGDFSDLSAFDERLQYIAEVCIFHSLAEDKI
BTS HHE3    661  RPVATIFKFKHKAISKDL-EFLDVESGKGLIDCDGTFIRQFIGRHFLLWGFYKAHSNAEDDI

FBXL5 HHE     65  IIGLLQQR-----SQTIYNVHSDNKLSEMLS-LFEKGLKNVKNEYEQL-----
BTS HHE1    112  IFSALDIR--VKNVAQTYSLHKGESNLFDH----LFE--LLNSATETDES-----
BTS HHE2    373  IFPAVDGE-----FSFSEEHDEEENQFNEFRC-LIE-NIKSAGASSTSA-----
BTS HHE3    720  LFPALESKETLHNVSHSYTLDHKQEEKLFGDIYSVLTELSILHEKLQSDSMEDIAQTDT

FBXL5 HHE    107  -----N-----YAKQLKERLEAFTRDFLPHMKEEEEVFQPMLMEYFT
BTS HHE1    155  -----YRRELARSTGALQTSVSQHLAKEQKQVFPLL-----
BTS HHE2    416  -----EFYTKLCSHADQIMETIQRHFHNEEIQVLPLARKNFS
BTS HHE3    780  VRTDIDNGDCNKKYNELATKLQGMCKSIKITLDQHIFLEELELWPLF-----

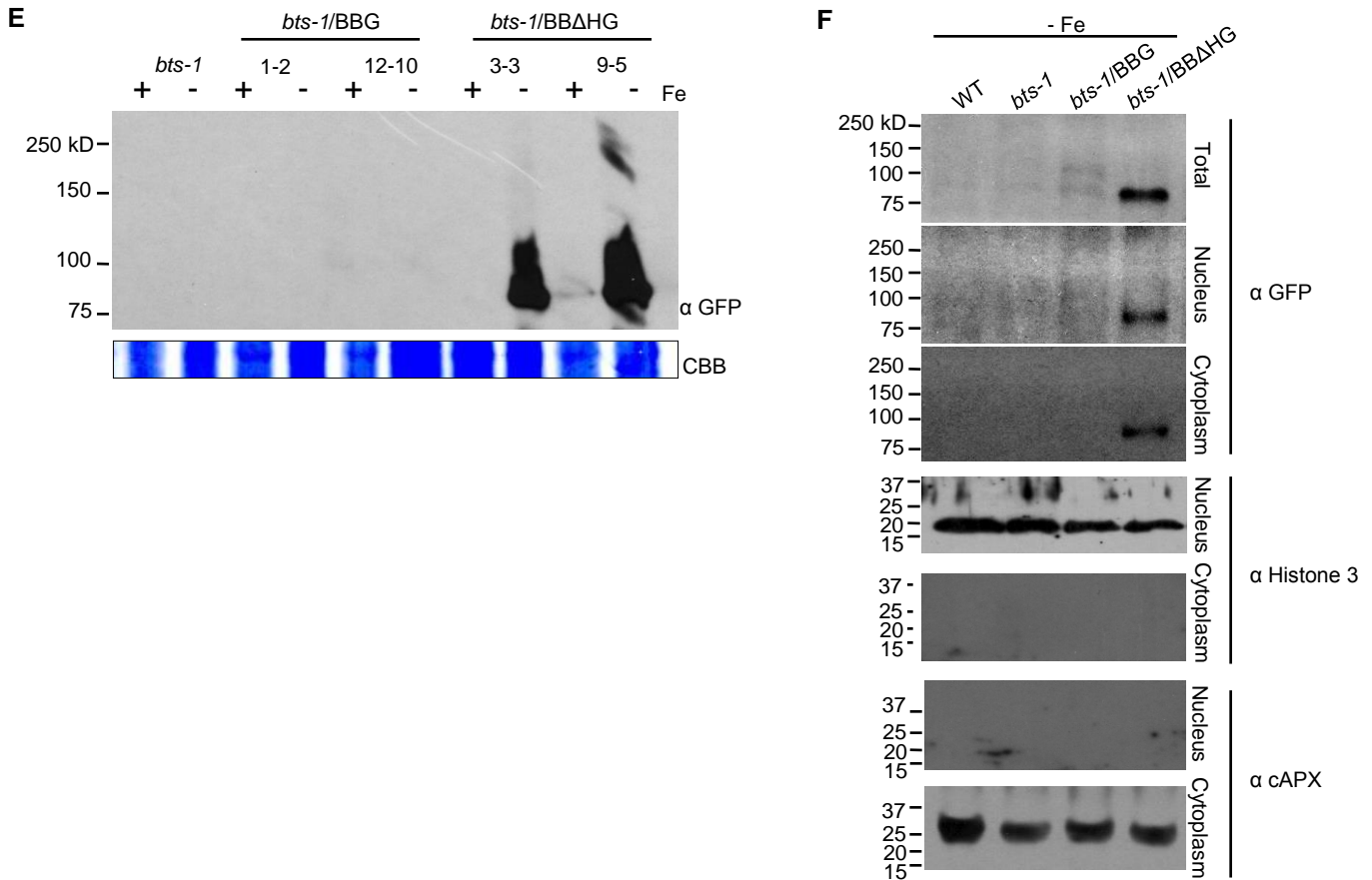
```

D



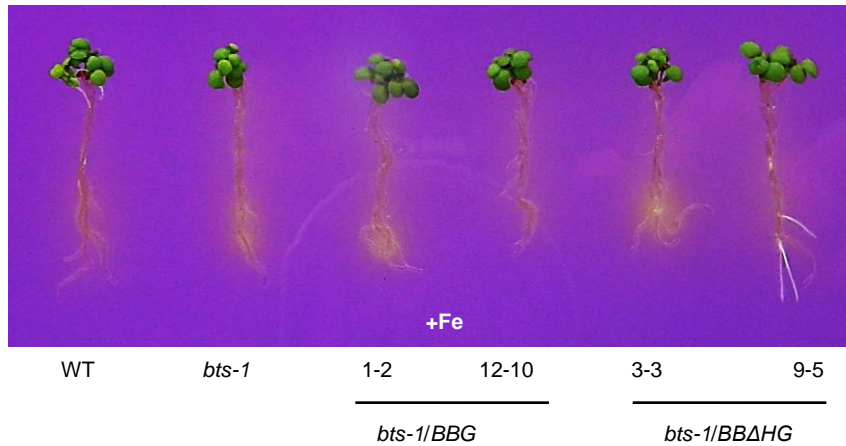
Supplemental Figure S8. In vivo and in vitro stability of BTS protein in the presence of iron. C, Alignment of mammalian FBXL5 and *A. thaliana* BTS HHE domains. Amino acids in black are identical. Glutamic acid (E) in bold red corresponds to single substitution E61A in FBXL5, which has been shown to eliminate iron-binding activity (Salahudeen et al., 2009) and used as reference to design BTS single substitutions, E108A, E369A and E716A, in HHE1, HHE2 and HHE3 domains respectively. Alignment created using Geneious 7.1.4 created by Biomatters. available from <http://www.geneious.com>. D, In vitro translation of 3xHA-tagged BTS, single amino acid substitutions (E108A, E369A and E416A) and triple amino acid substitution (Ex3A) BTS proteins were performed in presence of 400 μM DFO, and 400 μM FAC. Proteins were immunodetected using anti-BTS antibody. Amido Black staining indicates equal amount of wheat germ extract were loaded from in vitro protein translations. Results shown represent two independent assays.

Supplemental Figure S8



Supplemental Figure S8. *In vivo* and *in vitro* stability of BTS protein in the presence of iron. E, Stability of $BTS_{\Delta HHE}$ protein as compared to BTS protein in roots. Total protein extracted from 7-d-old (4 d +Fe and 3 d \pm Fe) *bts-1* seedlings expressing *ProBTS::BTS-GFP* (BBG) and *ProBTS::BTS $_{\Delta HHE}$ -GFP* (BBΔHG). Coomassie Brilliant Blue R250 (CBB) staining shows equal loading of protein. F, $BTS_{\Delta HHE}$ -GFP protein localization to the nucleus and cytoplasm in *A. thaliana* roots. Sub-cellular organelle fractionation was performed using sucrose-percoll discontinuous density gradient method from 7-d-old (4 d +Fe and 3 d -Fe) *bts-1* seedlings expressing *ProBTS::BTS-GFP* (BBG) and *ProBTS::BTS $_{\Delta HHE}$ -GFP* (BBΔHG). The immunoblots were re-probed with antibodies against nuclear (Histone 3) and cytoplasmic (cAscorbate Peroxidase, cAPX) protein to check purity of sub-cellular fractions.

Supplemental Figure S9



Supplemental Figure S9. Rhizosphere acidification of *bts-1* mutant lines complemented with BBG and BB Δ HG. 8-d-old seedlings of *bts-1/ProBTS::BTS-GFP* (BBG) and *bts-1/ProBTS::BTS Δ HHE-GFP* (BB Δ HG) were grown on +Fe media (4 d +Fe, 3 d +Fe and 1 d bromocresol purple). Eight plants per genotype were grouped on bromocresol purple agar medium. Results shown represent four independent assays.

Supplemental Table S1. List of primers

Primer Name	Gene Name	Gene ID	Purpose	Sequence
LbB1.3			genotyping	ATTTTGCCGATTTTCGGAAC
<i>bts-10L</i>	BTS	At3g18290	genotyping	AGAAATCTCTTCCGCGTCATC
<i>bts-10R</i>	BTS	At3g18290	genotyping	AGTAAACCTTGGAGCACATGC
<i>bts-12L</i>	BTS	At3g18290	genotyping	ATCGACATGGTGACCAGTAGC
<i>bts-12R</i>	BTS	At3g18290	genotyping	TTAGATTACGAACGGGTGCTG
<i>emb-2</i> LB1RP	BTS	At3g18290	genotyping	GCTTCCTATTATAAATTACCAATACA
<i>emb-2454-2LP</i>	BTS	At3g18290	genotyping	CGGTCACGTGCCAACCTGGG
<i>emb-2454-2RP</i>	BTS	At3g18290	genotyping	GGCGTCGCCATTTCCCCCAA
BTS_RT_2_F	BTS	At3g18290	qRT-PCR	GGACTCAACACTTGATCCGAGGAG
BTS_RT_2_R	BTS	At3g18290	qRT-PCR	CGGGGAACATCCAAGTTCAACATCACC
bTUB_RT_F	β -tubulin	At1g20010	qRT-PCR	CGACAATGAAGCTCTCTACGA
bTUB_RT_R	β -tubulin	At1g20010	qRT-PCR	AAGTCACACCGCTCATTGTT
BTS-MBP3_F	BTS	At3g18290	cloning	ATGGCGACGCCGTTACCAGAT
BTS-MBP2_R	BTS	At3g18290	cloning	CCACTCCTGCAGGTCAGGATG
bH115promFP_F	bHLH115	At1g51070	cloning	TGATTTTGGGGAAATTTTGAA
bH115promFP_R	bHLH115	At1g51070	cloning	CCAAAAGTCCAAAGCCAAGA
bH115promSP_F	bHLH115	At1g51070	cloning	GGGGACAACCTTTGTATAGAAAAGTTGTT AATCAACCAAATCCACTCTCTT
bH115promSP_R	bHLH115	At1g51070	cloning	GGGGACTGCTTTTTTTGTACAACTTGTC TCCTGATTCCCCGGCGGCTACT
bH105promFP_F	ILR3	At5g54680	cloning	CATTGCACCCGAATCTTCTT
bH105promFP_R	ILR3	At5g54680	cloning	CGGAACCCTAATTTGAAGCA
bH105promSP_F	ILR3	At5g54680	cloning	GGGGACAACCTTTGTATAGAAAAGTTGGG GAAAGAAAAGAGAGATGGATTT
bH105promSP_R	ILR3	At5g54680	cloning	GGGGACTGCTTTTTTTGTACAACTTGCT CCGGAACTTCCACCGGTGAAAA
115_QRTGFP_LP	bHLH115	At1g51070	qRT-PCR	TCATGCCTCCTGCTGCTG
115_QRTGFP_RP	bHLH115	At1g51070	qRT-PCR	CACCATCTAATTCAACAAGAATTG
ILR3_QRTGFP_LP	ILR3	At5g54680	qRT-PCR	GCCTCCTGCTTCAGTCGATA
ILR3_QRTGFP_RP	ILR3	At5g54680	qRT-PCR	TTGTGCCCATTAACATCACC
BTS_5primeSC_L_F	BTS	At3g18290	cloning	CACCTGAATGGCGACGCCGTTACC
BTS-SC-R	BTS	At3g18290	cloning	TCAGGATGAGGTTGAGCAGTCCGGG